Zamfir, M.; Patrickios, C.S.; Montagne, F.; Abetz, C.; Abetz, V.;
Oss-Ronen, L.; Talmon, Y.:

Styrene–vinyl pyridine diblock copolymers: Synthesis by RAFT polymerization and self-assembly in solution and in the bulk

In: Journal of Polymer Science A (2012) Wiley

DOI: 10.1002/pola.25935

Styrene – Vinyl Pyridine Diblock Copolymers: Synthesis by RAFT Polymerization and Self-assembly in Solution and in the Bulk

Mirela Zamfir,[1,†,§] Costas S. Patrickios,[1,*] Franck Montagne,[2] Clarissa Abetz,[3] Volker Abetz,[3] Liat Oss-Ronen[4] and Yeshayahu Talmon[4]

[1] Department of Chemistry
University of Cyprus
P. O. Box 20537
1678 Nicosia
Cyprus

[2] Division of Nanotechnology & Life Sciences
Swiss Center for Electronics and Microtechnology SA (CSEM SA)
CH 2002 Neuchâtel
Switzerland

[3] Institute of Polymer Research
Helmholtz-Zentrum Geesthacht
Max-Planck-Str. 1
21502 Geesthacht
Germany

[4] Department of Chemical Engineering
Technion-Israel Institute of Technology
Haifa 32000
Israel

Submitted for publication in

The Journal of Polymer Science, Part A: Polymer Chemistry

September 2011

Revised: December 2011

e-mail addresses:

Mirela Elena Zamfir:	mirela.zamfir@ics-cnrs.unistra.fr
Costas S. Patrickios:	costasp@ucy.ac.cy
Franck Montagne:	franck.montagne@csem.ch
Clarissa Abetz:	clarissa.abetz@hzg.de
Volker Abetz:	volker.abetz@hzg.de
Liat Oss-Ronen:	oss@techunix.technion.ac.il
Yeshayahu Talmon:	ishi@techunix.technion.il

[†] Present address: Precision Macromolecular Chemistry Group, Institut Charles Sadron, UPR22-CNRS, 23, rue du Loess, BP 84047, 67034 Strasbourg Cedex 2, France.

[§] Permanent address: Photochemistry Department, Petru Poni Institute of Macromolecular Chemistry, 41 A Gr. Ghica Voda Alley, 700487 Iasi, Romania.

* Author to whom correspondence should be addressed; tel. no: +357 22892768; fax no.: +357 22892801; e-mail: costasp@ucy.ac.cy

ABSTRACT

Reversible addition-fragmentation chain transfer (RAFT) polymerization along with benzyl dithiobenzoate chain transfer agent was employed for the controlled preparation of four diblock copolymers of styrene (St, less polar monomer) and 2- or 4-vinyl pyridine (2VP or 4VP, more polar monomers): St_{161}-*b*-$2VP_{48}$, St_{161}-*b*-$2VP_{121}$, St_{161}-*b*-$4VP_{76}$ and St_{161}-*b*-$4VP_{107}$, where the subscripts indicate the experimentally determined degrees of polymerization for each block. These diblock copolymers and their common homopolySt precursor were characterized in terms of their molecular weights and compositions using gel permeation chromatography and ^{1}H-NMR spectroscopy, respectively. All four diblock copolymers self-assembled in dilute toluene solutions to form reverse spherical micelles, which were characterized using atomic force microscopy and cryogenic transmission electron microscopy. Both microscopy techniques revealed that the 4VP-bearing diblock copolymers formed larger micelles than the 2VP-bearing ones, a result of the greater 4VP-toluene incompatibility as compared to the 2VP-toluene one. Finally, films cast from chloroform solutions of the diblocks were investigated in terms of their bulk morphologies using transmission electron microscopy. While the 2VP-containing block copolymer self-assembled into a spherical morphology, the 4VP-containing one with comparable composition and molecular weight formed a cylindrical structure, manifesting the greater 4VP-St incompatibility as compared to that of the 2VP-St pair.

Keywords: Diblock copolymers; reversible addition-fragmentation chain transfer polymerization; styrene; 2-vinyl pyridine; 4-vinyl pyridine; self-assembly; micelles; bulk morphologies.

1. INTRODUCTION

Block copolymers (BCs) are important self-assembling systems that can assume a wide diversity of nanometer-scale morphologies, including lamellar, hexagonally-packed cylindrical and body-centered cubic structures, due to the incompatibility and the connectivity constraints between the chemically distinct segments. This self-organization property of the BCs along with their large size have led to diverse applications in solution, in the bulk and in thin films.[1-3] Up to now, the technique most frequently used for the synthesis of BCs has been living anionic polymerization. However, anionic polymerization has to be carried out in complete exclusion of moisture and air and often at very low temperature. Furthermore, this polymerization technique is restricted to a relatively small number of monomers.[4] In order to overcome these limitations, efforts in the past two decades were focused on developing alternate techniques for BC synthesis.

Controlled radical polymerization techniques, such as nitroxide-mediated polymerization (NMP),[5,6] atom transfer radical polymerization (ATRP)[7,8] and reversible addition-fragmentation chain transfer (RAFT) polymerization,[9] are now available and provide themselves as facile and convenient means for the synthesis of block, graft, star, hyperbranched, telechelic and cyclic (co)polymers.[10] These polymers can be readily reactivated for chain extension with the same or different monomer since they retain their active end groups. RAFT polymerization possesses distinct advantages over the two other controlled radical polymerization techniques, including the absence of particular limitations in the reaction conditions, such as temperature and solvent, and, most importantly, the compatibility with a wide range of monomer type (methacrylates, acrylates, styrenics and acrylamides) and monomer functionality (carboxylic acid, carboxylic acid salt, hydroxyl or tertiary amine groups).[11]

BCs of styrene (St) and 4-vinyl pyridine (4VP) or 2-vinyl pyridine (2VP) represent an important class of polymers, as they can be used for the compatibilization of blends of the corresponding homopolymers via interfacial BC adsorption, ultimately leading to the enhancement of the mechanical properties of the blend,[12,13] or for the fabrication of functional nanostructures due to their potential use as templates and scaffolds.[14,15] Another attractive application of this type of BCs is the formation of organic ultrathin

nanoporous PSt-*b*-P4VP membranes for separation purposes (water treatment and filtration of biological entities), by a solution casting process, followed by the immersion of the cast film into a precipitant for the BC, which involves exchange of solvent with non-solvent in the solution film. This procedure leads to a thin and dense isoporous layer on top of a sponge-like porous support made of the same material.[16] Moreover, silicon-based nanoporous membranes with a precise control of the size and size-distribution of the nanopores, as well as the final thickness of the membranes, were produced by a proprietary process combining PSt-*b*-P2VP BC lithography and standard microfabrication techniques.[17]

Only a few papers have been published on the investigation of the synthesis of St-VP BCs using RAFT polymerization. In the first such study, Yuan and coworkers[18] described the preparation of various St-4VP-St or 4VP-St-4VP triblock copolymers using dibenzyl trithiocarbonate as chain transfer agent (CTA). These BCs, having molecular weights (MWs) in the range of 18000-29900 g mol^{-1} and 4VP mol fractions from 0.32 to 0.55, were characterized in terms of their self-assembly behavior in water. Zhang et al[19] reported the preparation of nanocomposites of montmorillonite (MMT) and PSt-*b*-poly(quaternized 4VP) (PSt-*b*-QP4VP) of number-average molecular weight (M_n) equal to 7400 g mol^{-1}, previously synthesized using RAFT polymerization, followed by quaternization of the 4VP units using CH_3I. Lately, a facile strategy for the preparation of multi-morphologies and a variety of nanostructures in solution was attained by the RAFT polymerization of St using a trithiocarbonate-terminated P4VP macroRAFT CTA (M_n=10400 g mol^{-1}) in methanol (selective solvent for PSt), by varying the feed molar ratios and controlling the polymerization conditions.[20]

Herein, we report the synthesis by RAFT copolymerization of four well-defined linear amphiphilic diblock copolymers of St and 4VP or 2VP, obtained by stepwise monomer addition, using benzyl dithiobenzoate (BDTB) as CTA. Following standard MW and composition characterization, the resulting BCs were thoroughly characterized in terms of their self-assembly behavior in solution and in the bulk.

2. EXPERIMENTAL SECTION

2.1. Materials

Styrene (St, purity > 99%), 2-vinyl pyridine (2VP, purity > 97%), 4-vinyl pyridine (4VP, purity > 95%), basic alumina, calcium hydride (CaH_2, 90-95%), 2,2-diphenyl-1-picrylhydrazyl hydrate (DPPH, 95%), *S*-(thiobenzoyl)thioglycolic acid (99%), benzyl mercaptan (99%), diethyl ether (99.7%) silica gel (60 Å, 70-230 mesh), *n*-hexane (96%), *N*,*N*-dimethylformamide (DMF, 99.8%), *N*,*N*-dimethylacetamide (DMAc, HPLC, ≥ 99.9%) were purchased from Aldrich, Germany. 2,2′-Azobis(isobutyronitrile) (AIBN, 95%), ethanol (99.6%), and deuterated chloroform ($CDCl_3$) were purchased from Merck, Germany. Tetrahydrofuran (THF, 99.8%, both HPLC and reagent grade) and methanol (99.9%) were purchased from Labscan, Ireland. The synthesis of BDTB is described in a following paragraph.

2.2. Methods

The monomers were passed through basic alumina columns to remove the inhibitors and any other acidic impurities. Subsequently, the DPPH free radical inhibitor was added to the monomers to prevent their undesired thermal polymerization. Afterwards, CaH_2 was also added, over which the monomers were stirred overnight to remove the last traces of moisture. This was followed by monomer vacuum distillation prior to their polymerization. The AIBN radical initiator was recrystallized twice from ethanol. The polymerization solvent, DMF, was dried over CaH_2 and filtered through syringe filters prior to use. Figure 1 displays the chemical structures and the names of the monomers, the initiator and the monofunctional CTA used for the diblock copolymer synthesis.

2.3. Syntheses

2.3.1. Synthesis of Benzyl Dithiobenzoate (BDTB)

BDTB was synthesized according to the published literature procedure.[21] In particular, 3.22 mL of benzyl mercaptan (3.41 g, 27.5 mmol) was added dropwise over a period of 30 minutes to a well-stirred dilute alkaline solution containing *ca.* 2 equivalents of NaOH (2 g in 200 mL H_2O, 50 mmol) and 5.3 g (25 mmol) of *S*-(thiobenzoyl)thioglycolic acid, keeping the reaction mixture at room temperature.

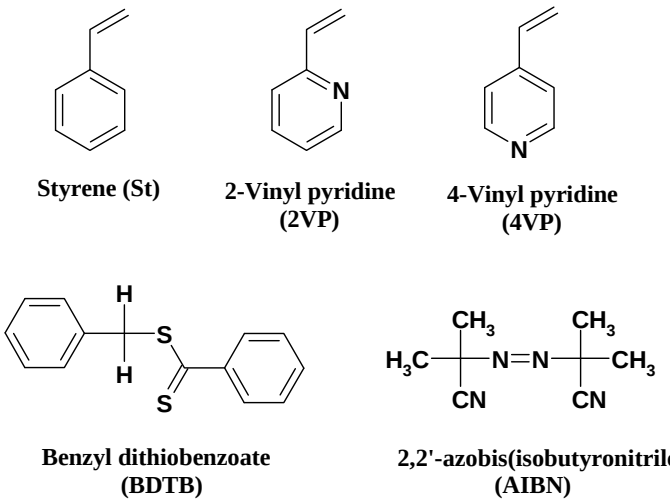

Figure 1. Chemical structures and names of the main reagents used for the diblock copolymer synthesis.

After 15 hours, BDTB separated out as a heavy, dark red oil and was extracted with ether (1 × 300 mL, 1 × 200 mL). The organic extracts were separately washed with 0.1 N aqueous NaOH (3 × 200 mL) and water (3 × 200 mL), and then dried over anhydrous $MgSO_4$. After the evaporation of the solvent, the remaining product was purified by column chromatography (silica gel, eluent: *n*-hexane). The purified CTA was stored in the freezer in the dark. ^{1}H-NMR (300 MHz, $CDCl_3$, 25 °C): δ = 4.6 ppm (2H, s, -C*H*$_2$-Ph), 7.29-7.99 ppm (10H, m, Ph); ^{13}C-NMR ($CDCl_3$, 25 °C): δ = 227.2 ppm (*C*=S), 144.7 ppm, 134.92-132.4 ppm, 129.27-126.87 ppm (Ph), 42.26 ppm (-S*C*H$_2$Ph). Yield: 81%.

2.3.2. Synthesis of Linear PSt MacroRAFT Agent

The synthetic procedure followed for the preparation of the PSt macroRAFT CTA with a targeted degree of polymerization (DP) equal to 300 is described in detail below. A mixture of St (25 mL, 22.72 g, 0.218 mol), BDTB (0.177 g, 0.728 mmol), and AIBN (74.5 mg, 0.454 mmol) were added into a 50 mL Schlenk tube equipped with a magnetic stirring bar and sealed with a rubber septum. After the mixture was degassed by three freeze-evacuate-thaw cycles, pure nitrogen gas was introduced into the tube which was subsequently immersed in an oil bath thermostated at 110 °C for 5 h. The polymerization was stopped by placing the tube in an ice bath. The tube was opened and the rather solid reaction mixture was dissolved in THF. The resulting THF solution was then slowly poured into an excess of methanol under stirring in order to precipitate the polymer. The precipitate was collected by filtration and dried

in a vacuum oven at room temperature for 36 hours. The PSt macroRAFT CTA was obtained at 66% yield and had an $M_{n(GPC)}$ = 16800 g mol^{-1} and a polydispersity index (PDI) = M_w/M_n = 1.4.

The polymerization reaction was followed kinetically. Samples were withdrawn at different reaction times. The monomer-to-polymer conversion was determined by ^{1}H-NMR spectroscopy from the ratio of the areas of the peaks of the olefinic protons of the monomer (5.18, 5.7, 6.6 ppm) divided by that of the aliphatic protons of the polymer (1.35-1.77 ppm), whereas the polymer MWs and PDIs were characterized by gel permeation chromatography (GPC).

2.3.3. Synthesis of Linear Block Copolymers PSt-*b*-PVP

Into a 25 mL Schlenk tube, 1.7 g of PSt macroRAFT CTA (0.101 mmol), 2VP or 4VP (1.75 mL, 1.71 g, 16.3 mmol) and DMF (3.5 mL) were added. After the mixture was degassed by three freeze-evacuate-thaw cycles, and placed under an inert nitrogen atmosphere, the tube was immersed in an oil bath thermostated at 80 °C. After the prescribed polymerization time (8 h for St_{161}-*b*-$2VP_{48}$, 19 h for St_{161}-*b*-$2VP_{121}$, 20 h for St_{161}-*b*-$4VP_{76}$ and 45 h for St_{161}-*b*-$4VP_{107}$; subscripts denote the experimentally determined degrees of polymerization), the tube was cooled down at room temperature immediately. The reaction mixtures were diluted with THF for the 2VP-containing BCs or with DMF for the 4VP-containing BCs, and the resulting BC solutions were slowly poured into excess of *n*-hexane to precipitate the produced BCs. After being separated by filtration and dried in a vacuum oven at room temperature for 24 h, the pure BCs were obtained as light pink glassy material.

2.4. Characterization

Gel Permeation Chromatography (GPC). All BCs and their PSt precursor were characterized using GPC to determine their MWs and their molecular weight distributions (MWD). For the PSt precursor and the 2VP-containing BCs, GPC was performed on a Polymer Laboratories chromatograph equipped with an ERC-7515A refractive index detector and a PL Mixed "D" column, calibrated using poly(methyl methacrylate) (PMMA) MW standards. The mobile phase was THF delivered at a flow rate of 1 mL min^{-1} using a Waters 515 isocratic pump. The MW calibration curve was based on eight narrow MWD linear PMMA standards (MWs of 850, 2810,

4900, 11 550, 30 530, 60 150, 138 500, and 342 900 g mol^{-1}) also from Polymer Laboratories. Since the P4VP blocks are insoluble in THF, their resultant BCs were analyzed in DMAc with LiCl as an additive (0.05 mol L^{-1}) at 50 °C, at a flow rate of 1 mL min^{-1} employing a set of two PSS 10 μ GRAM-Gel columns (3000 and 1000 Å, 8 × 300 mm each), and calibrated using PSt MW standards. A Knauer RI differential refractometer was used as a concentration detector. 20 μL of polymer solutions (0.2 wt.% in the mobile phase) were injected using a Rheodyne 7725i manual injection valve. Eluograms were flow-rate corrected using the method of internal standard (250 ppm diethylene glycol). Apparent molar mass averages, M_n and M_w, were based on PSt calibration and were calculated using the WinGPC software package (PSS GmbH, Mainz, Germany).

Proton and Carbon Nuclear Magnetic Resonance (^{1}H and ^{13}C-NMR) Spectroscopy. All BCs and their PSt precursor were also characterized by ^{1}H-NMR spectroscopy in terms of their composition and purity using a 300 MHz Avance Bruker NMR spectrometer equipped with an Ultrashield magnet, and using deuterated chloroform ($CDCl_3$) as solvent. The BDTB CTA was also characterized by ^{1}H and ^{13}C-NMR spectroscopy to confirm its structure and purity.

Transmission Electron Microscopy (TEM). TEM measurements were carried out using an FEI Tecnai G2 F20 transmission electron microscope operated at 200 kV in bright-field mode. All the samples were cast from 5 wt.% solutions in chloroform, following a standard procedure described below. The BC was dissolved in $CHCl_3$ and transferred into a Teflon dish inside a desiccator rich in solvent vapors. The overall evaporation (casting) procedure lasted for a period of two weeks. The samples were taken out of the crucibles and transferred in a vacuum oven in order to completely remove any traces of solvent and were treated thermally. The samples were dried for 8 h under vacuum at room temperature and then heated up to 40 °C using a rate of 10 °C h^{-1}, where they were stored for another 24 h. The last step involved their storage at 60 °C for 18 h. Afterwards, the oven was left to cool down to room temperature, the vacuum was released and the samples were taken out. Microtoming was performed at room temperature using a Leica Ultracut UCT microtome equipped with a Diatome Diamond Knife - Ultra 35°, the final sample thickness being approximately 50 nm.

Cryogenic-Transmission Electron Microscopy (cryo-TEM). Vitrified specimens of BC solutions in toluene (concentrations 0.2 to 1.0 w/v%) were prepared in the following manner. A drop of the solution was applied to a perforated carbon film supported on a TEM copper grid in a controlled environment vitrification system (CEVS). The CEVS is a closed chamber, which allows the maintaining of a constant temperature (25 °C for our experiments) and 100% saturation of the desired solvent (toluene in the present case), to prevent evaporation of the solution from the grid. Then, the drop was blotted to create a thin film (<300 nm) and immediately plunged into liquid nitrogen. The specimens were transferred to a Gatan 626 cooling holder via its transfer station and equilibrated in the microscope at about –180 °C. The samples were observed in a FEI T12 G2 transmission electron microscope operated in 120 kV low dose mode to minimize electron-beam radiation damage. We used Gatan US1000 high-resolution cooled-CCD camera to record the images at a nominal underfocus of 1 to 2 μm using the Digital Micrograph software package.

Atomic Force Microscopy (AFM). All the samples were characterized using AFM in the tapping mode with a Veeco Dimension 3100 microscope using silicon cantilevers (NSC15) from MikroMasch. Topography images were zero-order flattened using a standard algorithm from the Nanoscope III software. The preparation of micellar solutions and deposition on silicon substrates were performed as follows. The P2VP-containing BCs were dissolved in toluene at room temperature at a concentration of 0.2 wt.%. On the other hand, the P4VP-containing BCs were only partially soluble in toluene at room temperature and were, therefore, heated up to 80 °C for 30 min and then cooled down to room temperature under stirring. All micellar solutions were filtered through PTFE syringe filters with 0.45 μm pore diameters. Prior to micelle deposition, 1 cm^2 silicon substrates were cleaned in a piranha solution (H_2O_2 : H_2SO_4, 1:3 v/v%) at 120 °C for 30 min, rinsed in boiling deionized water for 20 min and dried with nitrogen (*Caution: Piranha solution is a hazardous oxidizing agent and must be handled with extreme care*). Micellar films were spin-coated at 4000 rpm for 30 s in a chamber of controlled atmosphere (T = 21 °C and 60% of relative humidity).

3. RESULTS AND DISCUSSION

Amphiphilic BCs of St and 2VP or 4VP were synthesized via BDTB-mediated RAFT polymerization, according to Scheme 1.

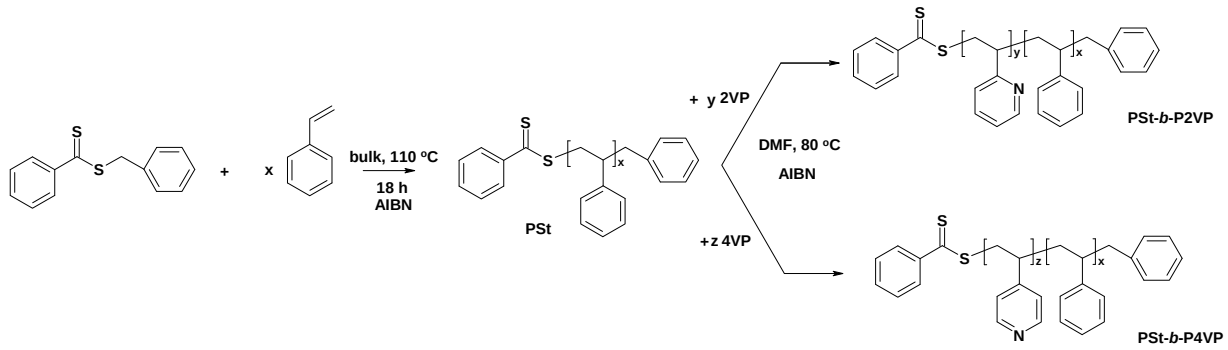

Scheme 1. Synthetic route followed for the preparation of the St-2VP and St-4VP diblock copolymers via RAFT polymerization.

3.1. Styrene Homopolymer

The polymerization of St was performed at 110 °C in the bulk, with BDTB as the RAFT CTA and AIBN as the initiator ($[St]_0$ / $[CTA]_0$ / $[AIBN]_0$ = 300 : 1 : 0.625), to yield a polymer having an M_n value equal to 16800 g mol^{-1} and a PDI of 1.4. The successful formation of the linear homopolymer precursor was also confirmed by ^{1}H-NMR spectroscopy. In particular, resonance signals assigned to the aliphatic protons of the hydrocarbon backbone of the polymer appeared in the range of 1.35 - 1.77 ppm, whereas the intensity of the peaks due to the St olefinic protons at 5.18, 5.7, 6.6 ppm was greatly reduced.

The reaction was followed kinetically. The monomer conversion and the polymer M_n and PDI in the samples extracted at various reaction times were determined. Figure 2 presents the collected kinetic data in different plots. In particular, Figure 2 shows (a) the temporal evolution of St conversion (calculated from the ^{1}H-NMR spectra), (b) the dependence of M_n on monomer conversion, (c) the temporal evolution of M_n, the MW at the peak maximum (M_p) and the PDI, and (d) the pseudo-first-order kinetic plot for monomer conversion. The linearity of the M_n variation *vs.* monomer conversion plot and of the ln([M_0/M]) *vs.* time plot, are both good indications of the controlled character of the polymerization. Figure 2(b) shows that the M_n values as determined by GPC were slightly lower (by ~10%) than those expected on the basis of monomer conversion. This indicates that no CTA deactivation took place, which

would have led to higher M_n values as compared to the theoretical ones; it also indicates some experimental errors in the determination of M_n by GPC, in the determination of monomer conversion by ^{1}H NMR spectroscopy, and in the determination of the mass of the CTA used for the polymerization.

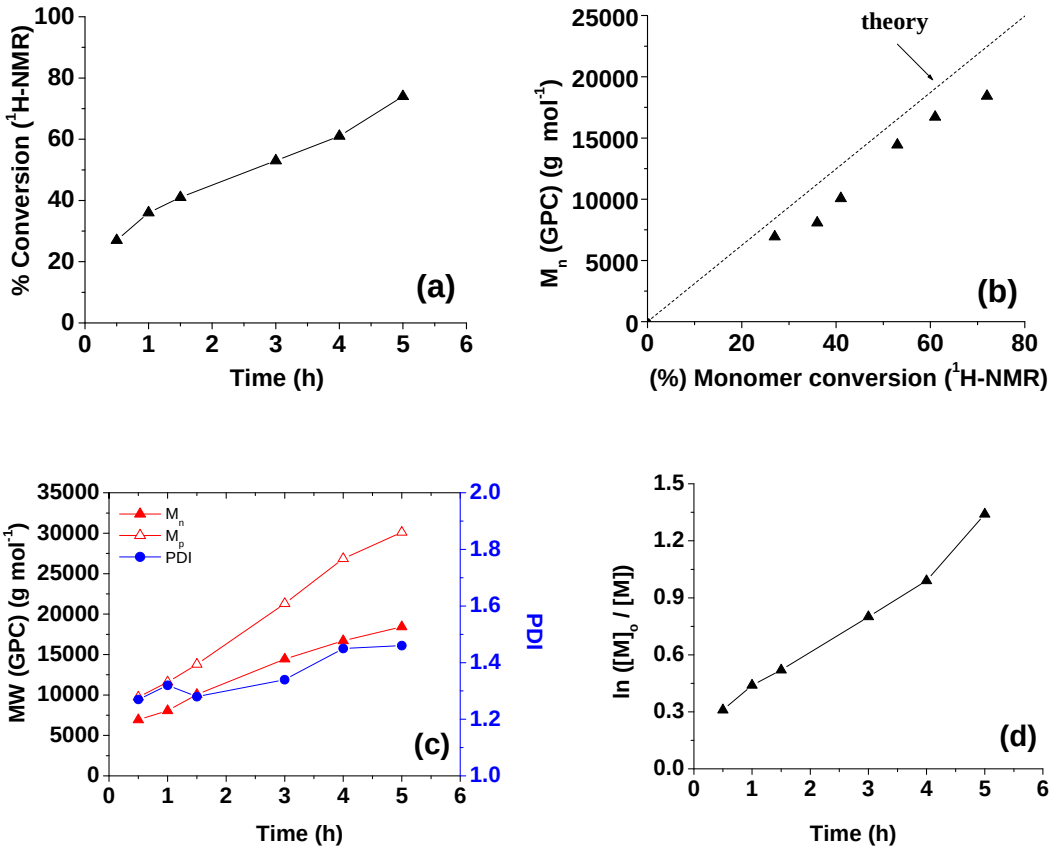

Figure 2. Results of the kinetic study of styrene RAFT homopolymerization. (a) Temporal evolution of the conversion of styrene, (b) dependence of M_n on monomer conversion, (c) temporal evolution of the MWs and the PDIs, and (d) pseudo-first-order kinetic plot of the polymerization. $[St]_0 : [AIBN]_0 : [CTA]_0 = 300 : 0.625 : 1$, temperature = 110 °C, bulk polymerization.

3.2. Diblock Copolymers

The four diblock copolymers of this investigation, St_{161}-*b*-$2VP_{48}$, St_{161}-*b*-$2VP_{121}$, St_{161}-*b*-$4VP_{76}$ and St_{161}-*b*-$4VP_{107}$, were synthesized by chain-extending the same PSt macroRAFT CTA with 2VP or 4VP in DMF, using AIBN as initiator at 80 °C for 8 to 45 h. Typical ^{1}H-NMR spectra of (A) the PSt macroRAFT CTA, (B) the BC St_{161}-*b*-$2VP_{48}$ and (C) the BC St_{161}-*b*-$4VP_{107}$ are shown in Figure 3. The VP content in the copolymers was calculated from the ratio of the peak area of the "c" protons at position 3 of the pyridine ring (8.3-8.4 ppm), divided by the area of peaks "b"

corresponding to all backbone methylene and methine protons (1.4-1.8 ppm). Using this copolymer composition and the GPC-determined M_n of the PSt homopolymer precursor, another estimation of the copolymer MW was made. Table 1 lists the yields, the size, and the composition characteristics of the starting homopolymer and its daughter diblock copolymers.

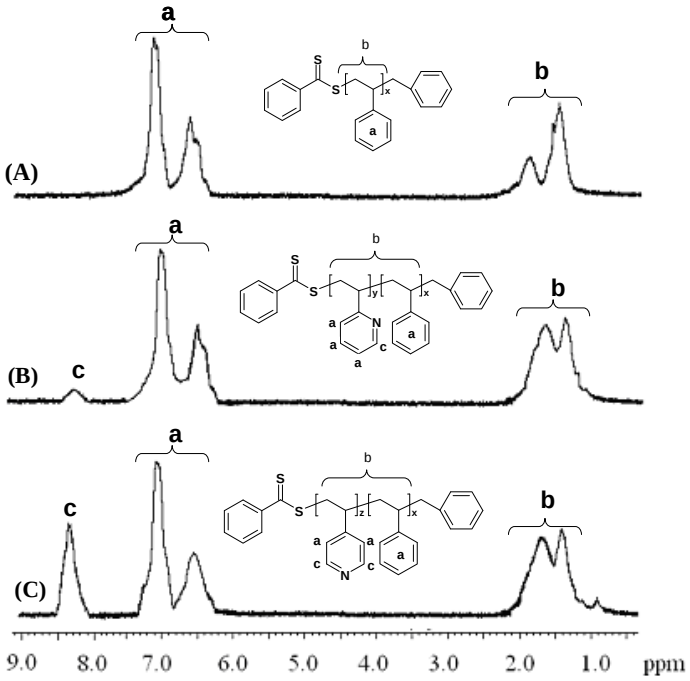

Figure 3. ^{1}H-NMR spectra of (A) the PSt macroRAFT CTA, (B) St_{161}-*b*-$2VP_{48}$ and (C) St_{161}-*b*-$4VP_{107}$, all recorded in $CDCl_3$.

Table 1. Monomer conversions, polymer compositions, molar masses and PDIs for the St homopolymer and St-VP BCs synthesized in this study.

Sample	CTA	VP content (mol%)	Time (h)	Conv[c] (%)	M_n		PDI	Yield[d] (%)
					GPC	NMR		
St_{161}[a]	BDTB	0	18	70	16800	-	1.44	66
St_{161}-*b*-$2VP_{48}$[b]	St_{161}	23	8	28	21000	21800	1.71	71
St_{161}-*b*-$2VP_{121}$[b]		43	19	58	22300	29500	1.71	76
St_{161}-*b*-$4VP_{76}$[b]		32	20	77	26300	24700	1.55	73
St_{161}-*b*-$4VP_{107}$[b]		40	45	83	25900	28000	1.68	76

[a] Polymerization at 110 °C in the bulk and at $[CTA]_0/[St]_0/[AIBN]_0 = 1/300/0.625$.
[b] Second-stage polymerization at 80 °C in DMF and at $[CTA]_0/[VP]_0/[AIBN]_0 = 1/160/0.625$.
[c] Conversions were determined from the ^{1}H-NMR spectra.
[d] Gravimetric yield.

The controlled nature of the polymerizations in this study is also demonstrated in Figure 4 which displays the GPC traces of the St homopolymer and the two St-2VP

BCs produced using the former as a macroRAFT CTA. It may be observed that the GPC traces of the BCs were shifted to shorter elution times and the MWDs were broadened relative to the parent PSt macroRAFT CTA (corresponding to increases in the PDI values from the original value of 1.4 for the parent St homopolymer to 1.7 for the BCs, Table 1). This increase in PDI reflects the tailing toward lower MWs in the MWDs of the BCs, resulting from deactivated polymer generated during the synthesis of the macroRAFT CTA.[22.23] This can be produced by an unfavorable high concentration of radicals responsible for a substantial extent of termination reactions.[24]

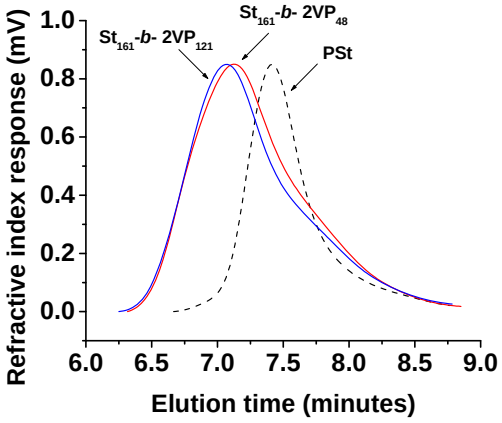

Figure 4. GPC traces of the St_{161} macroRAFT CTA and the daughter diblock copolymers St_{161}-*b*-$2VP_{48}$ and St_{161}-*b*-$2VP_{121}$.

The GPC traces of St_{161}-*b*-$4VP_{76}$ and St_{161}-*b*-$4VP_{107}$ BCs (not shown) were recorded using DMAc as solvent, due to the insolubility of P4VP in THF.[25] The peaks were shifted to higher MWs, from 16800 g mol^{-1} to 26300 g mol^{-1} and 25900 g mol^{-1}, while the PDIs of the BCs increased from 1.4 to 1.6 and to 1.7. The GPC traces revealed a bimodal MWD with the high MW shoulder indicating partial recombination of the polymer chains.

The greater polarity and reactivity of 4VP over that of 2VP are the likely reasons for the more extensive side reactions in the block copolymerizations of the former compared to those of the latter, leading to bimodal MWDs in the diblocks with 4VP and only a tail in those with 2VP. These side reactions were more pronounced in the present investigation, where relatively high MWs were targeted in order to afford readily microphase-separating block copolymers. The deactivated polymer in the GPC traces in Figure 4 is PSt with just a small number of 2VP units.

Self-assembly Behavior in Solution and in the Bulk

Reverse Micelles in Toluene. It is well known that amphiphilic BCs form micelles or reverse micelles when dissolved in selective solvents. Regular micelles are formed in aqueous or in high polarity solvents, while reverse micelles are formed in non-polar or in low-polarity solvents.[26] In this study, the low-polarity selective solvent toluene was chosen, and, therefore, reverse micelles were expected to form. Toluene solutions of all four BCs were characterized using AFM and cryoTEM. The results are presented and discussed below.

For the AFM measurements, BC solutions in toluene were deposited onto a silicon substrate, and let dry. The recorded images are presented in Figure 5. The reverse micelles formed were characterized in terms of their height (h in nm), mean diameter (ϕ in nm) and adsorption density (in number of micelles per μm^2). Due to the spreading of the micelles upon their adsorption onto the substrate, and due to characterization in the dry state, it is expected that $h << \phi$. Both of the 2VP-containing diblock copolymers formed spherical micelles with the same characteristics in terms of the h and the ϕ values, 3 nm and 23 nm, respectively, with differences being observed only for the density of the deposited micelles (Figure 5a, 5b). Thus, in the case of the St_{161}-*b*- $2VP_{121}$ BC, comprising a higher content of insoluble core block, the density of the micelles was found to be lower ($150/\mu m^2$) as compared to St_{161}-*b*-$2VP_{48}$ ($224/\mu m^2$). This was most likely due to the fact that a longer solvophobic block resulted in greater aggregation numbers, producing a smaller number of larger micelles.

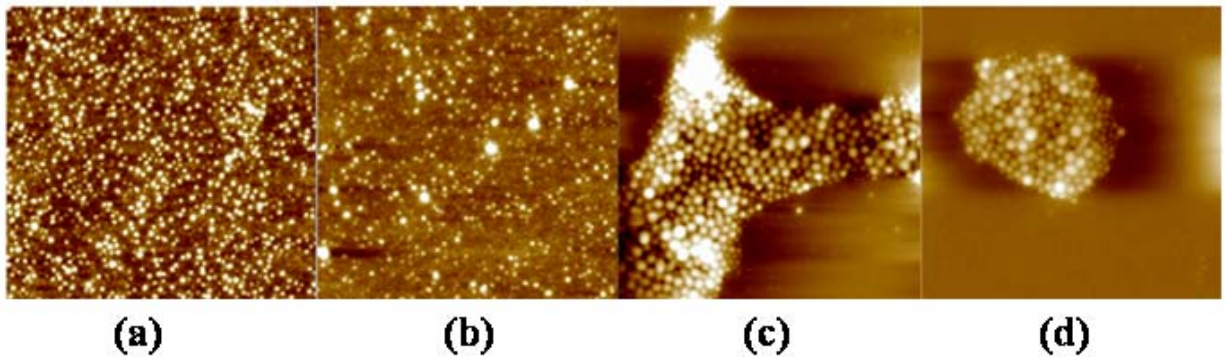

Figure 5. Topographic tapping-mode AFM images (2 μm × 2 μm scan size) of the reverse micelles formed by the BCs cast from toluene solution (C = 0.2 w/v%) (a) St_{161}-*b*-$2VP_{48}$ (3 nm), (b) St_{161}-*b*-$2VP_{121}$ (3 nm), (c) St_{161}-*b*-$4VP_{76}$ (10 nm) and (d) St_{161}-*b*-$4VP_{107}$ (17 nm). The values in parentheses indicate the micelle heights measured by AFM.

The P4VP-containing BCs exhibited greater micellar diameters and heights, 40 and 10 nm for St_{161}-*b*-$4VP_{76}$ and 59 and 17 nm for St_{161}-*b*-$4VP_{107}$, as compared to the P2VP-containing ones. This was due to the greater polarity of the P4VP block than the P2VP block, leading to a greater incompatibility with toluene and a stronger drive for (reverse) micellization in toluene in the case of the PSt-P4VP BCs as compared to the PSt-P2VP ones.[27] The BC with the longer solvophobic P4VP block formed larger (diameter and height) reverse micelles, as expected.

In addition to their larger size, the PSt-P4VP-based micelles presented a more heterogeneous spatial distribution on the silicon substrate than the PSt-P2VP-based ones. This is probably due to stronger interactions between the former type of micelles themselves, arising from their larger size in solution, rather than the stronger affinity of the 4VP block for the silicon substrate, as the present aggregates are reverse micelles with PVP cores shielded from the substrate by the PSt shells.

For the cryo-TEM imaging, BC solutions in toluene (concentrations 0.2 to 1.0 w/v%) were deposited onto perforated carbon films supported by copper grids, vitrified in liquid nitrogen, and imaged at about –180 °C in the TEM. This method allows direct imaging of the morphologies produced by the BCs in the bulk of the solution. Samples of the recorded images are presented in Figure 6. Micellar aggregates are clearly seen in the vitrified solution. 'C' denotes the carbon part of the perforated carbon films. The results are very similar to those obtained using AFM. In particular, the PSt-P4VP BCs formed larger reverse micelles than the PSt-P2VP ones, with the former exhibiting diameters of around 58 nm, whereas the latter having diameters of 22 nm. In most cases the micelles were globular and polydisperse in diameter; however, some more elongated micelles were also observed.

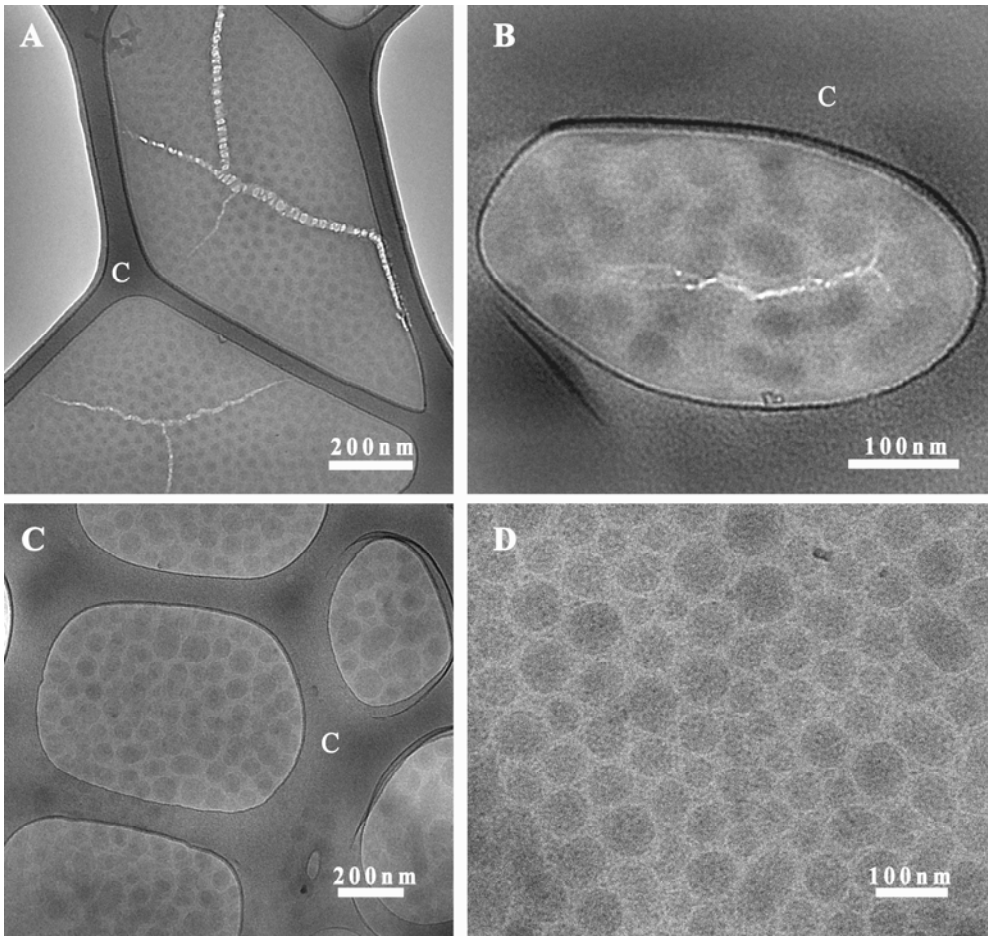

Figure 6. Cryo-TEM images of the reverse micelles formed by the BCs in toluene solutions. The letter 'C' denotes the perforated carbon film. (a) St_{161}-*b*-$2VP_{48}$ (*c* = 1.0 w/v%), (b) St_{161}-*b*-$2VP_{121}$ (*c* = 0.2 w/v%), (c) St_{161}-*b*-$4VP_{76}$ (*c* = 1.0 w/v%), and (d) St_{161}-*b*-$4VP_{107}$ (*c* = 1.0 w/v%).

Bulk Morphologies. BCs comprising monomers of sufficient mutual incompatibility and possessing high enough MW microphase separate in the bulk, and form composition-dependent morphologies. Films cast from chloroform solutions of BCs St_{161}-*b*-$2VP_{48}$ and St_{161}-*b*-$4VP_{76}$, having similar M_n values of around 25 000 g mol^{-1}, were investigated in terms of their bulk morphology using TEM, and the recorded images are displayed in Figure 7. While St_{161}-*b*-$2VP_{48}$ formed a spherical structure (Figure 7a), the St_{161}-*b*-$4VP_{76}$ diblock copolymer formed hexagonally packed cylinders of P4VP in a PSt matrix, coexisting with layered structures (Figures 7b and 7c); the latter corresponded to cylinders lying in the plane of the section.[28,29] The alternating light and dark bands suggest a layered morphology; the presence of light (PSt) channels extending into the dark (P4VP) layers demonstrate that this morphology is not lamellar. The spots in a hexagonal array correspond to an end-on

view of the cylinders and the layered structures correspond to a side view normal to the cylinder axis. The experimental value of the diameter of one cylinder was found to be 40 nm which compares favorably with the value of 38.3 nm calculated considering fully stretched P4VP blocks of number-average degree of polymerization of 76 (=2 × 76 × 0.252 nm[30]). However, given the BC PDI of almost 1.6, this would not necessarily imply fully stretched P4VP chains. The sphere formation in the St-2VP BC can be attributed to the lower polarity and weaker polarizability[29] of 2VP than 4VP, leading to a smaller incompatibility with St in the former case.

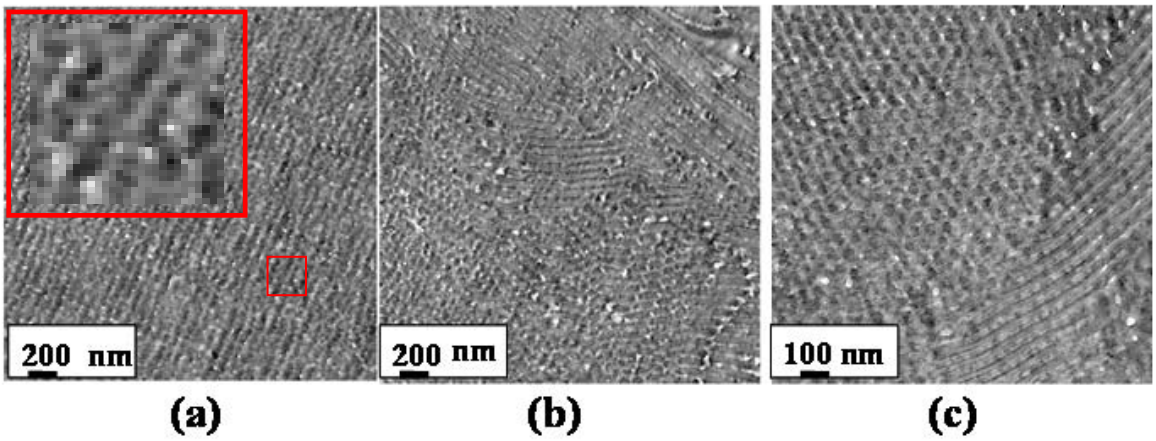

Figure 7. TEM images of (a) St_{161}-*b*-$2VP_{48}$, (b) and (c) St_{161}-*b*-$4VP_{76}$, cast from chloroform. The inset at the top-left corner of (a) is a 4 × 4 magnification of the area indicated towards the bottom-right corner of (a).

The spheres in Figure 7(a) are rather small and blurred due to the relatively low MW and high polydispersity of the St_{161}-*b*-$2VP_{48}$ BC. It is noteworthy that the 2VP volume fraction of this BC of 23% was expected to lead to cylinder, rather than sphere, formation. Thus, the observed spherical structure is apparently a non-equilibrium frozen morphology. In contrast, the St_{161}-*b*-$4VP_{76}$ BC, comprising the more PSt-incompatible P4VP block, and a 4VP volume fraction of 32%, further away from that for sphere formation (12%), readily equilibrated to cylinders.

4. CONCLUSIONS

RAFT step-wise copolymerization was employed for the synthesis of diblock copolymers of St and VP, two with 2VP and the other two with 4VP. In solution, all four diblock copolymers were able to self-assemble in the non-polar and selective solvent toluene to form reverse micelles. The copolymers with blocks comprising the

more polar 4VP units formed larger micelles than their 2VP-based counterparts of similar size and compositions, manifesting the greater driving force for self-assembly in the case of the former type of block copolymers. In the bulk, the diblock copolymer with the more PSt-incompatible P4VP block was able to microphase separate into hexagonally-packed cylinders, while the similar diblock with the less PSt-incompatible P2VP block formed a spherical structure.

ACKNOWLEDGEMENTS

The authors wish to thank the European Commission for funding this work within the FP7 project SELFMEM (Grant Agreement No. NMP3-SL-2009-228652). We are also grateful to Dr. P. F. W. Simon of the Helmholtz-Zentrum Geesthacht, for kindly recording for us the GPC traces for the P4VP-containing BCs. Furthermore, we are indebted to Dr. E. Kesselman of the Technion Israel Institute of Technology for her valuable suggestions and assistance with the cryo-TEM characterization of the samples. Finally, we are grateful to the A. G. Leventis Foundation for helping establish the NMR infrastructure at the University of Cyprus.

REFERENCES

1. Thomas, E. L.; Anderson, D. M.; Henkee, C. S.; Hoffman, D. *Nature* **1988**, *334*, 598.

2. Bates, F. S. *Science* **1991**, *251*, 898.

3. Hamley, I. W. P*rog. Polym. Sci.* **2009**, *34*, 1161.

4. Hsieh, H. L.; Quirk, R. P. *Anionic Polymerization: Principles and Practical Applications*; Marcel Dekker, Inc., New York, **1996**.

5. Sciannamea, V.; Jérôme, R.; Detrembleur, C. *Chem*. *Rev*. **2008**, *108*, 1104.

6. Hawker, C. J.; Bosman, A. W.; Harth, E. *Chem*. *Rev*. **2001**, *101*, 3661.

7. Kamigaito, M.; Ando, T.; Sawamoto, M. *Chem. Rev.* **2001**, *101*, 3689.

8. Matyjaszewski, K.; Xia, J. *Chem*. *Rev*. **2001**, *101*, 2921.

9. Rizzardo, E.; Chiefari, J.; Mayadunne, R.; Moad, G.; Thang, S. *Macromol*. *Symp*. **2001**, *174*, 209.

10. Matyjaszewski, K. *Macromol*. *Symp*. **2001**, *174*, 51.

11. Moad, G.; Rizzardo, E.; Thang, S. H. *Aust*. *J*. *Chem*. **2005**, *58*, 379.

12. Dai, C. A.; Dair, B. J.; Dai, K. H.; Ober, C. K.; Kramer, E. J.; Hui, C. Y.; Jelinski, L. W. *Phys*. *Rev*. *Lett*. **1994**, *73*, 2472.

13. Dai, C. A.; Jandt, K. D.; Dhamodharan, R.; Slack, N. L.; Dai, K. H.; Davidson, W. B.; Kramer E. J. *Macromolecules* **1997**, *30*, 549.

14. Cho, Y. H.; Yang, J. E.; Lee, J. S. *Mater*. *Sci*. *Eng*. **2004**, *24*, 293.

15. Yun, S. H.; Yoo, S. I.; Junc, S. C.; Sohn, B. H. *Chem*. *Mater*. **2006**, *18*, 5646.

16. Peinemann, K. V.; Abetz, V.; Simon, P. F. W. *Nat*. *Mater*. **2007**, *6*, 992.

17. Krishnamoorthy, S.; Pugin, R.; Brugger, J.; Heinzelmann, H.; Hinderling, K. *Adv*. *Funct*. *Mater.* **2006**, *16*, 1469.

18. Yuan, J. J.; Ma, R.; Gao, Q.; Wang, Y.-F.; Cheng, S.-Y.; Feng, L.-X.; Fan, Z.-Q.; Jiang, L. *J*. *Appl*. *Polym*. *Sci*. **2003**, *89*, 1017.

19. Zhang, B.-Q.; Chen, G.-D.; Pan, C.-Y.; Luan, B.; Hong, C.-Y. *J*. *Appl*. *Polym*. *Sci*. **2006**, *102*, 1950.

20. Wan, W.-M.; Hong, C.-Y.; Pan, C.-Y. *Chem. Commun.* **2009**, 5883.

21. Severac, R.; Lacroix-Desmazes, P.; Boutevin, B. *Polym. Int.* **2002**, *51*, 1117.

22. Goto, A.; Sato, K.; Tsujii, Y.; Fukuda, T.; Moad, G.; Rizzardo, E.; Thang, S. H. *Macromolecules* **2001**, *34*, 402.

23. Goto, A.; Fukuda, T. *Macromolecules* **1997**, *30*, 5183.

24. Wong, K. H.; Davis, T. P.; Barner-Kowollik, C.; Stenzel, M. H. *Polymer* **2007**, *48*, 4950.

25. Varshney, S. K.; Zhong, X. F.; Eisenberg, A. *Macromolecules* **1993***, 26,* 701.

26. Gohy, J.-F. *Adv. Polym. Sci.* **2005**, *190*, 65.

27. Liu, Y.; Lor, C.; Fu, Q.; Pan, D.; Ding, D.; Liu, J.; Lu, J. *J. Phys. Chem. C* **2010**, *114*, 5767.

28. Brandrup, J.; Immergut, E. H. *Polymer Handbook*, 3rd ed., Wiley: New York, 1989.

29. Zha, W.; Han, C. D.; Lee, D. H.; Han, S. H.; Kim, J. K.; Kang, J. H.; Park, C. *Macromolecules* **2007**, *40*, 2109.

30. Hiemenz, P. C. Polymer Chemistry: The Basic Concepts. New York: Marcel Dekker; 1984, p. 6.